Active nuclear import and cytoplasmic retention of Activation Induced Deaminase

Anne-Marie Patenaude[1], Alexandre Orthwein[1,2], Yi Hu[1,3], Vanina A Campo[1], Bodil Kavli[3], Alejandro Buschiazzo[4,5] and Javier M Di Noia[1,2,6]

[1]Institut de Recherches Cliniques de Montréal, 110 Av des Pins Ouest, Montréal, H2W 1R7, Canada.

[2]Department of Microbiology and Immunology, University of Montreal, Montreal, QC, Canada.

[3]Department of Cancer Research and Molecular Medicine, Norwegian University of Science and Technology, Erling Skjalgssons gt. 1, DMF, 7006 Trondheim, Norway.

[4]Institut Pasteur de Montevideo, Unidad de Cristalografia de Proteinas, Montevideo, Uruguay. Mataojo 2020, Montevideo 11400, Uruguay.

[5]Institut Pasteur, Département de Biologie Structurale & Chimie, Paris, France.

[6]Department of Medicine, University of Montreal, Montreal, QC, Canada.

a

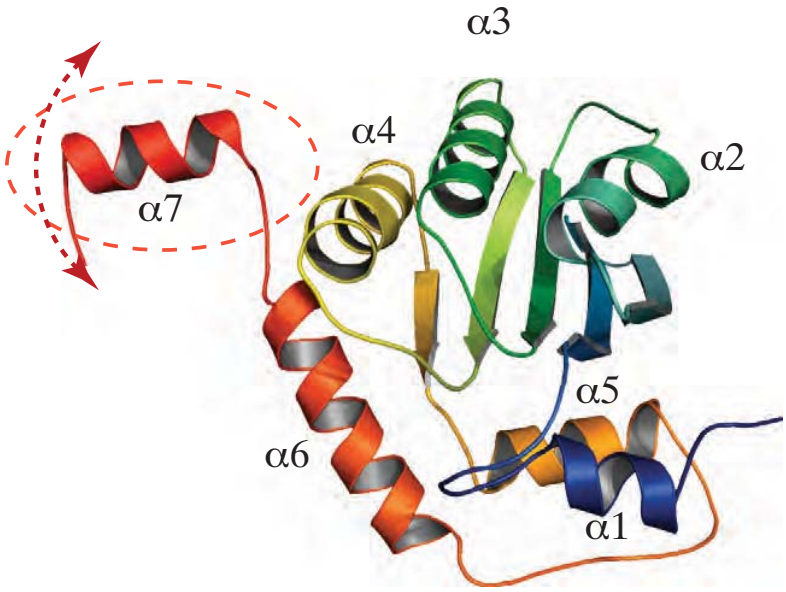

b

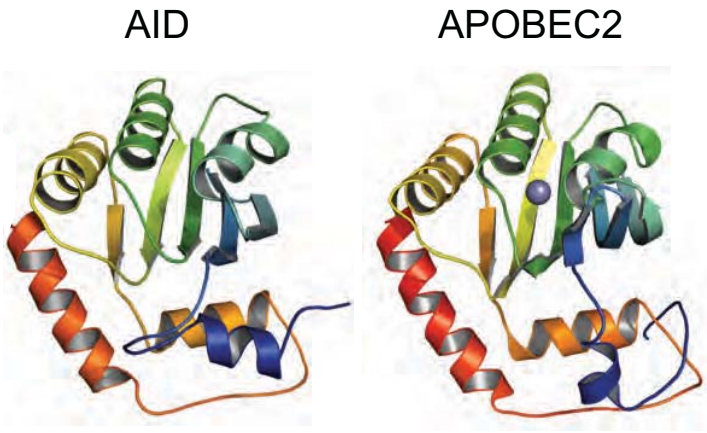

Supplementary Figure 1
(Di Noia)

Supplementary figure 1 Three dimensional model of AID. (**a**) Cartoon representation of a homology 3D model of AID, using structurally aligned 2NYT (APOBEC2), 3E1U and 2JYW (APOBEC3G C-terminal domain) as templates. APOBEC2 and AID share 31% identity and 50% similarity over the aligned regions. AID and APOBEC3G C-terminal domain share 45% identity and 61% similarity. The colors follow a blue-to-red ramp indicating N- to-C-terminal direction. Secondary structure elements are labeled in order from N- to C-terminus. The dotted ellipse encircles a predicted C-terminal α-helix (α7), which is not present in any experimental 3D model and distinguishes AID from its paralogs. The expected mobility of α7 is highlighted, poised to fold against the globular core of AID and/or other protein partners. The Zn^{++} atom (not shown) is predicted to be bound by residues at the converging N-termini of α-helices α2 and α3. (**b**) Comparison of the three-dimensional structure of APOBEC2 with the homology model of AID. A blue-to-red ramp indicates N-to-C-terminal direction. The Zn^{++} atom in the active site of APOBEC2 is depicted (purple sphere). The C-terminal 17 amino acids of AID are not represented.

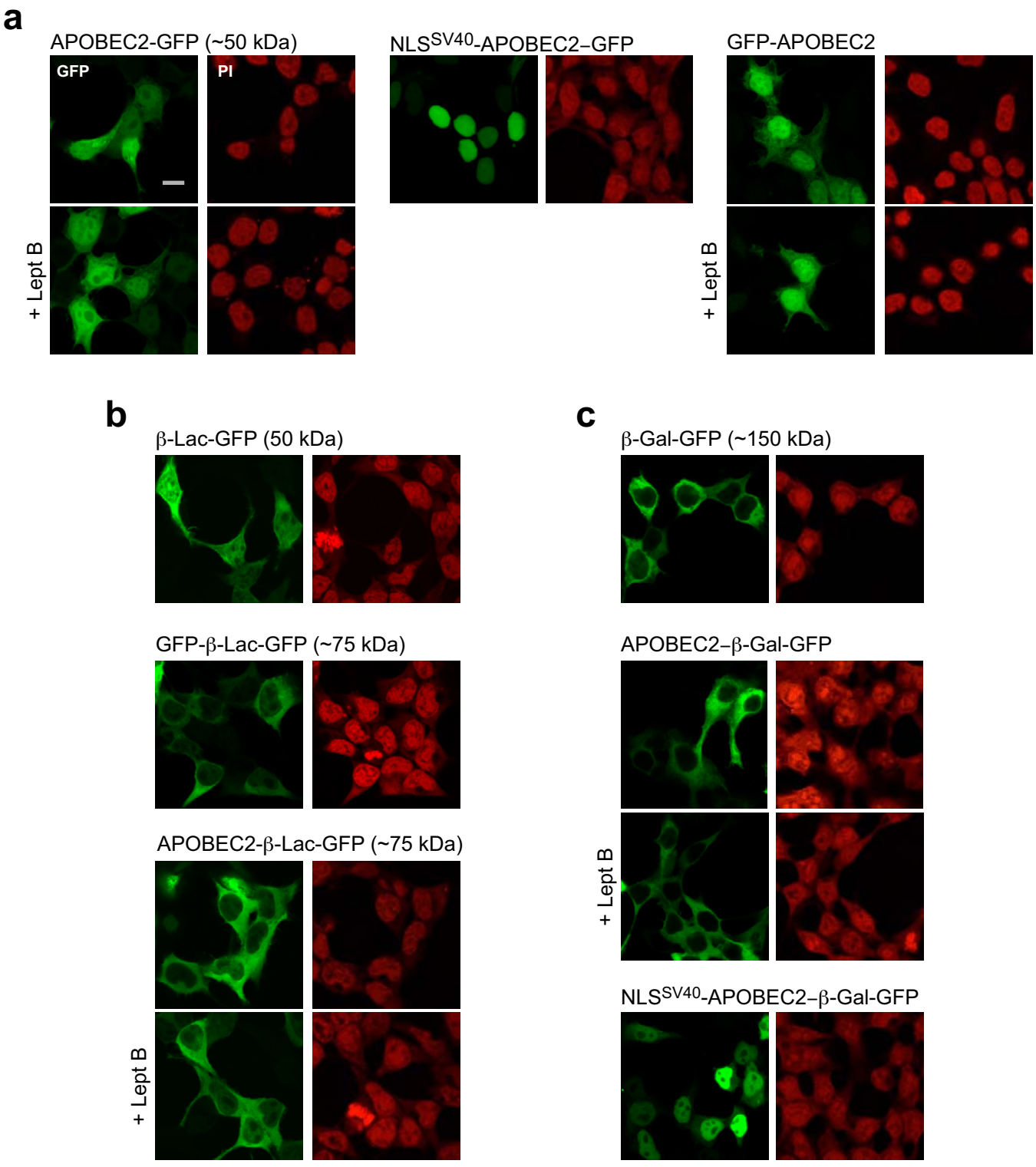

Supplementary Figure 2
(Di Noia)

Supplementary figure 2 APOBEC2 has no nuclear import or export information. Representative images of the indicated A2-GFP constructs transiently transfected in 293T cells. The labels indicate the actual order of the fragments in the fusion proteins. Where indicated the cells were treated with 50 ng ml^{-1} leptomycin B (+ Lept B) for 4 h before fixation and processing for confocal microscopy. Nuclei stained with propidium iodide (PI) are shown in red. Magnification, 630X. Bars, 10 μm. (**a**) A2-GFP localization is insensitive to leptomycin B treatment or the position of the GFP tag, but can be sent to the nucleus by NLS^{SV40}. (**b**) A2 is unable to mediate nuclear import as part of a 75 kDa protein. β-Lac (β-Lactamase)-GFP (~50 kDa) can diffuse across the nuclear membrane unless the size of the protein is increased to ~75 kDa by fusing another GFP molecule or A2, as a further indication that this size is still below the nuclear pore cut-off in these cells. (**c**) A2 is unable to mediate nuclear import as part of a 175 kDa protein. Similar experiments to those in **b** were done using β-Gal (β-Galactosidase)-GFP (~150 kDa). Fusing A2 did not cause any nuclear localization of this exclusively cytoplasmic protein. Further fusion of NLS^{SV40} fully transported the ~175 kDa protein into the nucleus.

These experiments show that A2 does not seem to have any detectable information for nuclear import or export, nor any retention mechanisms. Most of these constructs were assayed also in HeLa cells with identical results (data not shown).

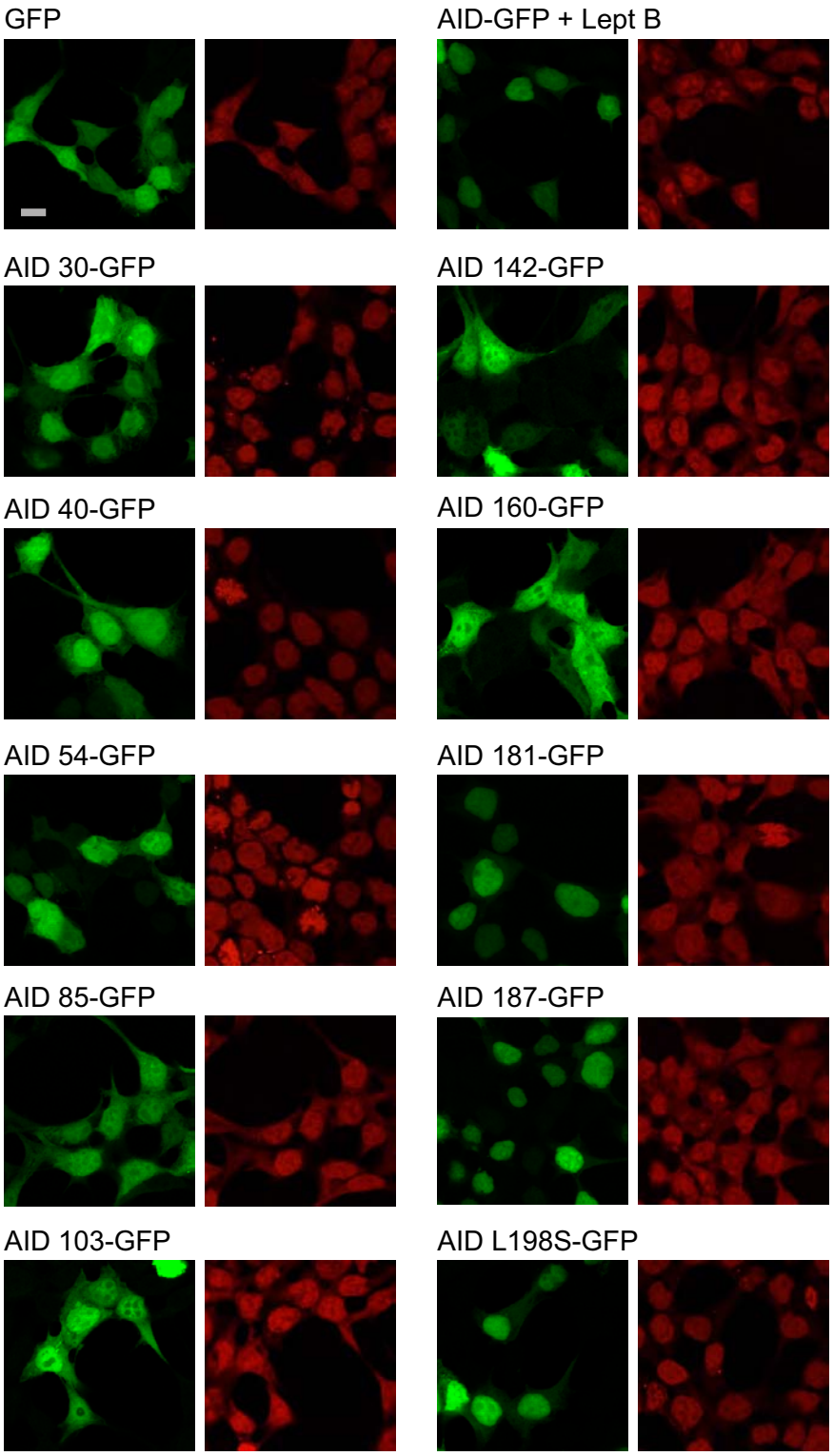

Supplementay Figure 3
(Di Noia)

Supplementary figure 3 Mapping of the minimal import-proficient fragment of AID in 293T cells. Representative confocal images showing the subcellular localization of GFP control, AID-GFP after leptomycin B treatment and AID-GFP variants bearing C-terminal truncations in transiently transfected 293T cells. Constructs are named according to the last residue of AID included. Nuclei are shown in red stained with propidium iodide. Magnification, 630X. Bars, 10 μm.

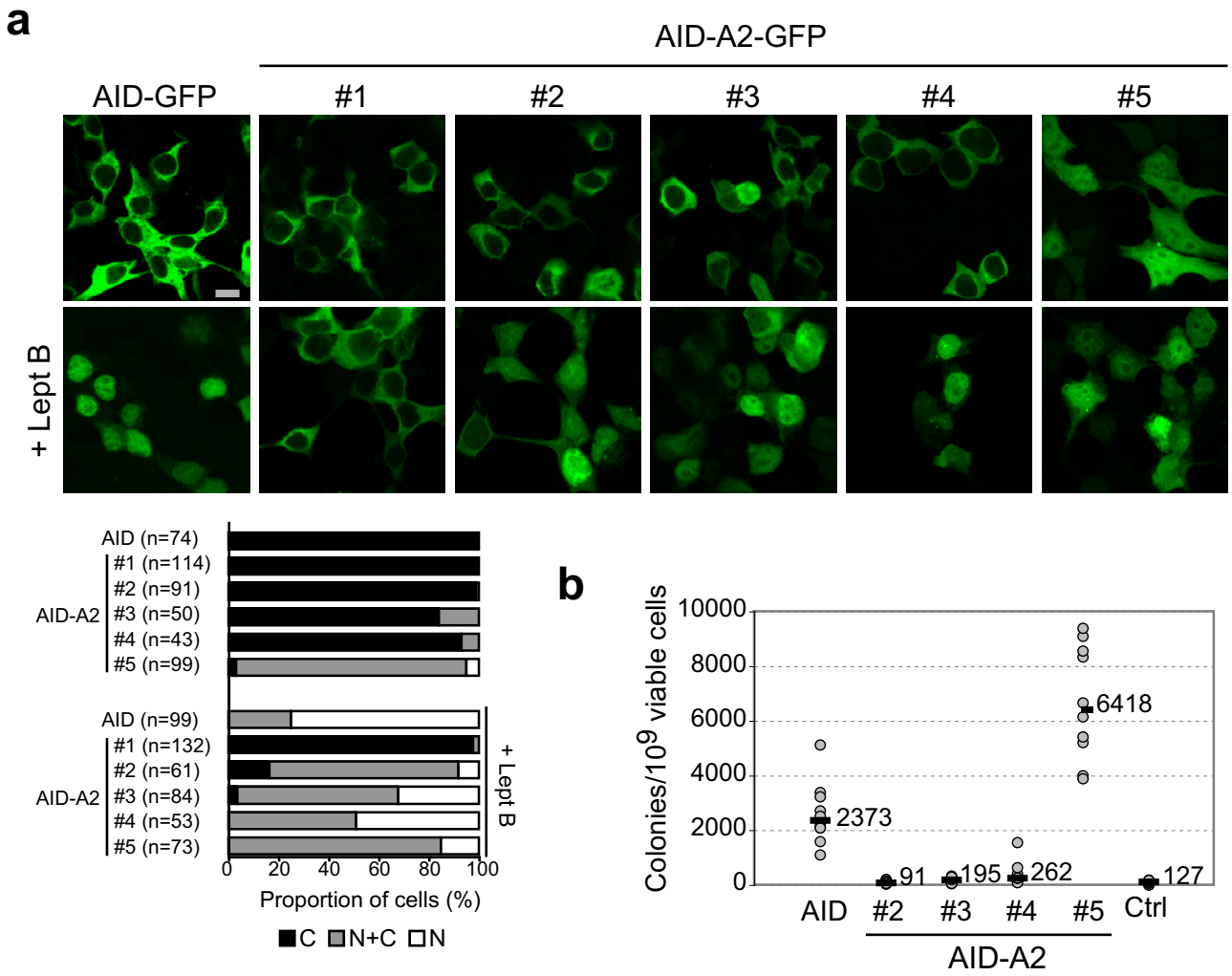

Supplementary Figure 4
(Di Noia)

Supplementary figure 4 Mapping of AID subcellular localization determinants using AID-APOBEC2 chimeras in 293T cells. (**a**) Representative confocal images of 293T cells transiently expressing AID or AID-A2 #1 to #5 fused to the N-terminus of GFP in the steady state and after 4 h incubation with 50 ng ml^{-1} of leptomycin B. Magdnification, 630X. Bars, 10 μm. The stacked bars plot below summarizes the scoring of the subcellular localization of AID-GFP control and AID-A2 #1 to #5-GFP in steady state and after leptomycin B treatment. Cells from 5-10 randomly picked fields from two independent experiments were counted and classified according to whether the GFP signal was cytoplasmic (black), homogeneous throughout the cell (grey) or largely nuclear (white). The total number of cells scored for each condition is indicated (*n*). (**b**) Mutation assay in *E coli* BW310 [*Δung*] showing that AID-A2 #5 is catalytically active. Data from two independent experiments are pooled and median values for all independent cultures are indicated. AID-A2 #1-GFP could not be expressed in *E coli*. (**c**) AID-A2 #5 cannot be actively imported into the nucleus. Representative confocal images of 293T cells transiently transfected with plasmids encoding AID-A2 #5-GFP or the larger variant #5-βGal-GFP. Magnification, 630X. Bars, 10 μm.

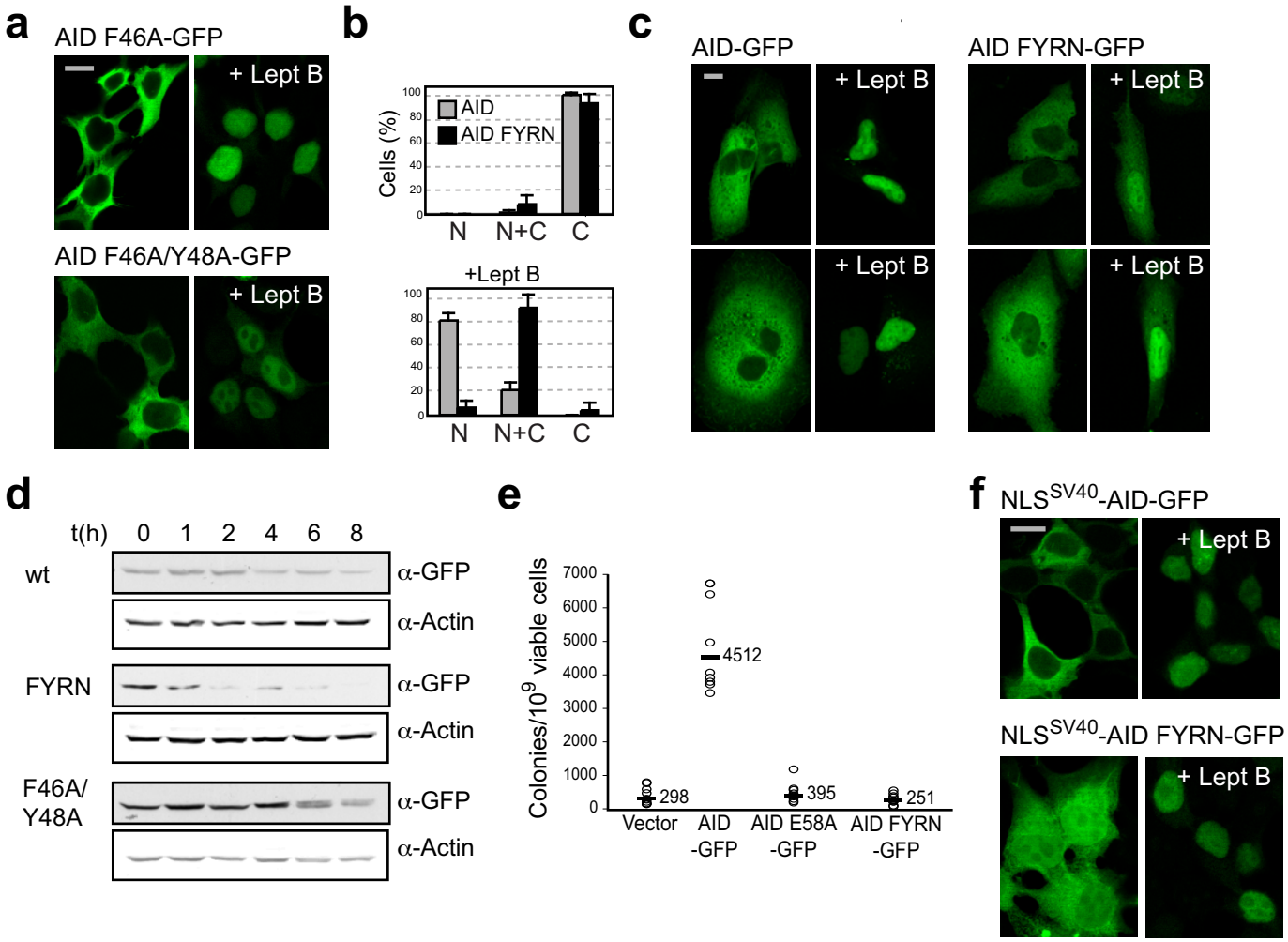

Supplementary Figure 5
(Di Noia)

Supplementary figure 5 Subcellular localization of AID mutants in predicted oligomerization surfaces suggest multiple and scattered nuclear import determinants. (**a**) Oligomerization proficient AID variants bearing mutations in β2 retain nuclear accumulation. Representative confocal images of 293T cells transiently transfected with plasmids encoding AID-GFP carrying the indicated mutations in the steady state or after leptomycin B treatment. (**b**) Bar plot summarizing the scoring of the subcellular localization for AID FYRN-GFP and AID-GFP in 293T cells in steady state and after leptomycin B treatment. Cells from randomly picked fields were counted and classified according to their predominant subcellular localization as largely cytoplasmic (C), homogeneous throughout the cell (N+C) or nuclear (N). Average + s.d. from multiple fields from three transfections are plotted. The total number of cells scored was AID *n*=87, AID FYRN *n*=99, AID + Lept B *n=206*, AID FYRN + Lept B *n*=160. (**c**) AID FYRN is also mislocalized in Hela cells. Representative confocal images of HeLa cells transiently transfected in parallel with plasmids encoding AID-GFP or the mutants AID FYRN (F46A/Y48A/R50G/N51A) in the steady state or after treatment with leptomycin B. (**d**) AID FYRN is unstable. Aliquots of 293T cells transiently transfected with plasmids encoding each of the indicated AID-GFP proteins were harvested at the indicated times after addition of cycloheximide, lyzed and analyzed by western blot with anti-GFP antibodies. Actin was used as loading controls. (**e**). Mutation assay in *E coli* BW310 [*Δung*] shows that AID FYRN is catalytically inactive. Data from two independent experiments are pooled, median values for all the independent cultures are indicated. (**f**) AID FYRN can be sent to the nucleus by an heterologous NLS. Representative confocal images of 293T cells transiently transfected with plasmids encoding AID-GFP and AID FYRN-GFP with an N-terminally fused NLS (from SV40 large T antigen) in steady state and after leptomycin B treatment. (**g**) Scattered basic residues influence AID nuclear import. Representative images of 293T and HeLa cells transiently transfected with plasmids encoding AID-GFP bearing the indicated mutations in the steady state or after treatment with leptomycin B. All pictures magnification, 630X. Bars, 10 μm.

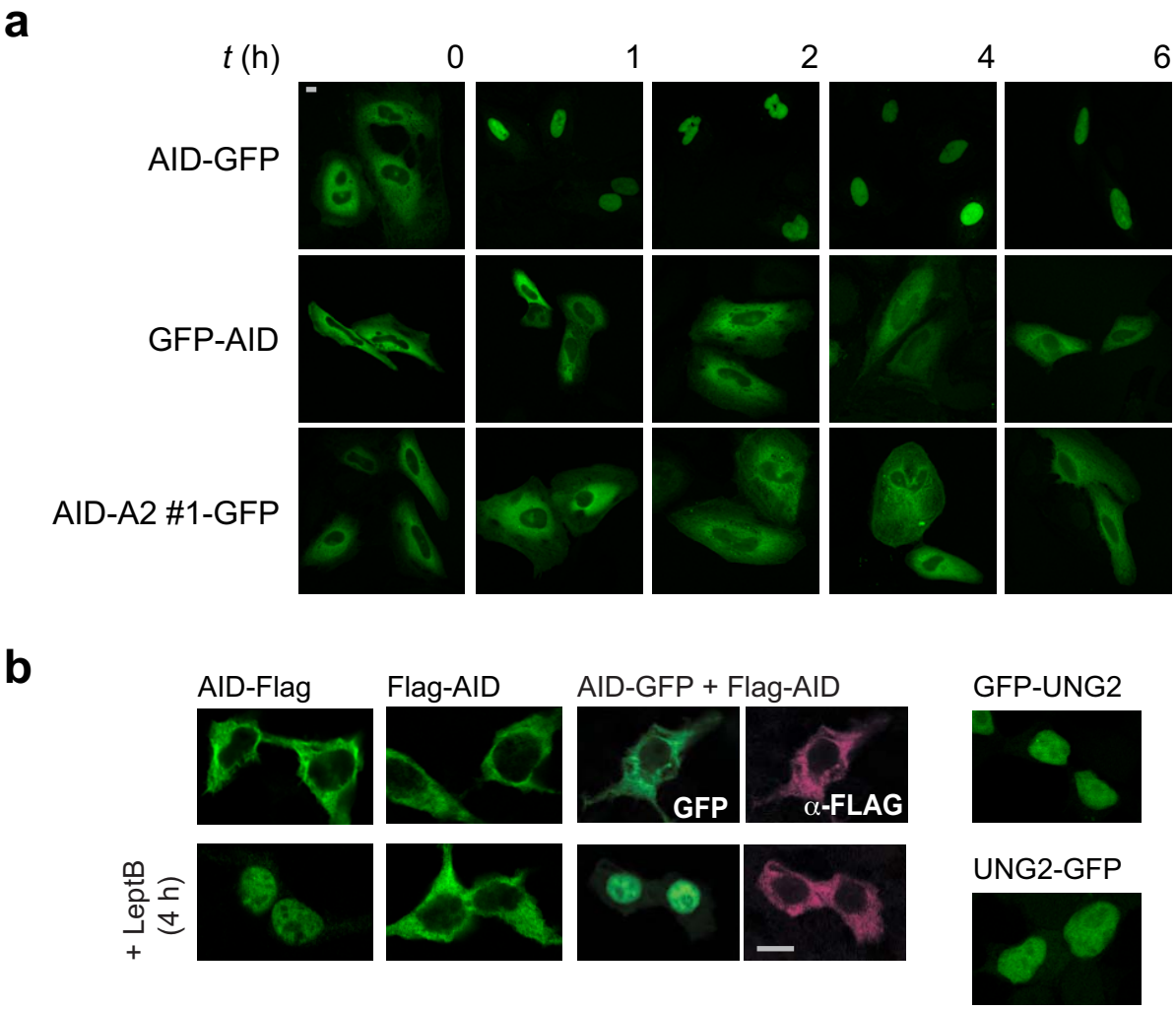

Supplementary Figure 6
(Di Noia)

Supplementary figure 6 N-terminal fusions of AID fail to diffuse into the nucleus but still oligemerize. (**a**) Representative confocal pictures of HeLa cells transiently expressing AID-GFP, GFP-AID or AID-A2 #1-GFP at different times after the addition of leptomycin B. (**b**) Representative confocal images of 293T cells transiently transfected with plasmids encoding Flag-AID, AID-Flag or cotransfected with Flag-AID and AID-GFP in the steady state or after leptomycin B treatment. Flag was detected using anti-Flag followed by anti-mouse AlexaFluor546 (pseudocolored). Representative confocal images of 293T cells transiently transfected with plasmids encoding UNG2-GFP and GFP-UNG2 are shown as controls that nuclear import is usually insensitive to the tagged protein end. UNG2, nuclear isoform of mouse uracil-DNA glycosylase. Magnification, 630X. Bars, 10 μm. (**c**) Oligomerization assay for the indicated AID variants. The fusion proteins indicated on the top were transiently coexpressed with AID-Flag. The ability of these proteins to coimmunoprecipitate with AID-Flag after anti-Flag pull-down was assessed by western blot.

The observation that AID-GFP does not bring Flag-AID into the nucleus when these proteins are able to oligomerize in coIP assays may at first glance suggest that oligomerization is not necessary for import. Alternatively, this observation may just reflect dynamic oligomerization between AID-GFP and Flag-AID with heterodimers being less efficiently imported. Since AID-GFP homodimers would be removed from the equation once they enter the nucleus in the presence of leptomycin B, it could lead to the observed phenotype. In addition, we discuss the possibility that C-terminal tags may affect retention, just as N-terminal tags affect import. This is suggested by slower nuclear accumulation of untagged AID as compared to AID-GFP in response to leptomycin B. In cotransfected cells, AID-GFP would be preferentially imported and Flag-AID preferentially retained, contributing to the observed phenotype.

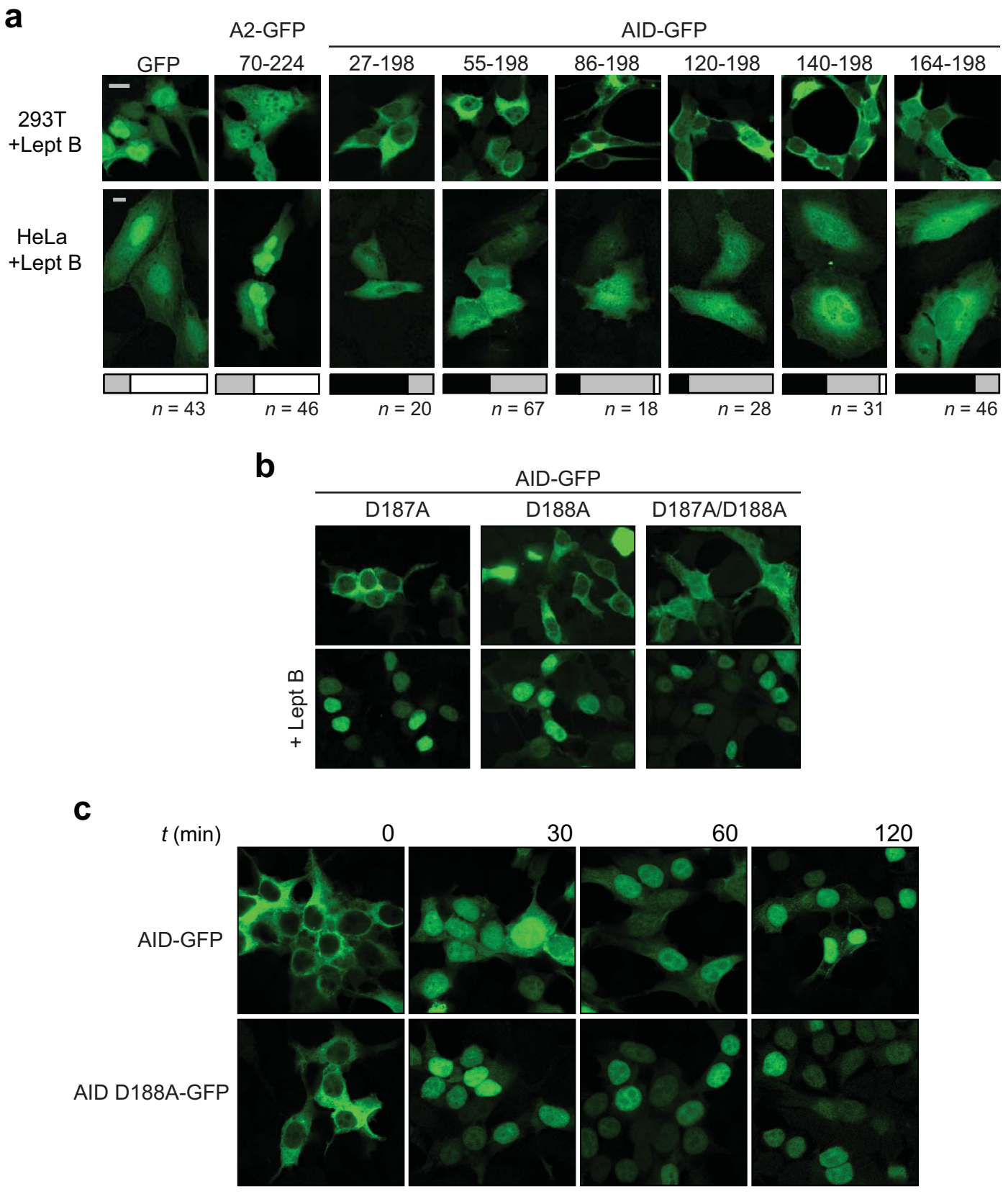

Supplementary Figure 7
(Di Noia)

Supplementary figure 7 Cytoplasmic retention mutants and N-terminal truncations of AID. (**a**) The C-terminal domain of AID, but not the one of A2, is able to restrict the diffusion of GFP from the cytoplasm of 293T and Hela cells. The collection of AID-GFP variants with N-terminal truncations resulting in AID fragments encompassing the indicated residues, were analyzed for subcellular localization in 293T and Hela cells treated with leptomycin B. Representative confocal pictures of 293T cells show that all the AID constructs are retained in the cytoplasm while the A2 control construct has the same distribution as GFP. In Hela cells, all constructs are more nuclear than in 293T, consistently with the differences observed between these two cell types for other constructs. Still, all AID constructs show a clearly different subcellular localization (more cytoplasmic) than the control A2 construct, which again shows the same distribution as GFP. This is well apparent when Hela cells from multiple fields from 2 independent experiments are simply scored based on the relative signal intensities in nucleus as compared to cytoplasm (C>N, C=N or C<N), which is summarized in the stacked bars plots belw each corresponding picture. This result strongly supports that the C-terminal region of AID mediates a delay in diffusion, especially when compared to the C-terminal truncations shown in supplementary figure 3. (**b**) Both Asp187 and Asp188 collaborate in AID cytoplasmic retention. Simultaneous mutations D187A/D188A (but not each single mutations) disrupts nuclear exclusion of AID-GFP in 293T cells. Representative images of 293T cells transiently transfected with the indicated AID-GFP mutants. (**c**) Representative confocal pictures of 293T cells transfected with AID-GFP and AID D188A-GFP at different time points after leptomycin B treatment. For all pictures magnification, 630X. Bars, 10 μm.

Supplementary table 1 – Summary of subcellular localization of AID mutants

	Construct	Localization[1]		Activity		Affects[12]
		Steady state	+ Lept B	Catalytic[2]	CSR	(I, E, R)
AID	wt	C	N	1	++	-
	R19A	C	C+N/C>N[3]	0.2 (R19E)[4]	ND	I
	R24W	C	C+N	- (R24E)[4]	-[5]	I
	F46A	C	N	0.4[6]	+[6]	-
	F46A/Y48A	C	N	0.2[4]	ND	-
	F46A/Y48A/R50G/N51A	C	C+N	-	-	I
	R112D	C	C+N/C>N[3]	- (R112C) [4]	-[7]	I
	Y114A/F115A	C	N	0.2[5]	ND	-
	E117A/D118A	C	N	ND	ND	-
	R178A	C	N	ND	ND	-
	Y184A	C	N	ND	++/-[8]	-
	Y184D	C	N	ND	ND	-
	E185A	C	N	ND	ND	-
	D187A	C+N/C[3]	N	ND	ND	R
	D188A	C+N/C[3]	N	ND	-	R
	D187A/D188A	C+N	N	1.1	-	R
	R190A	C	N	ND	++[9]	-
	D191A	C	N	ND	++/-[9]	-
	L198S	N	N	1.7 (F198S)[10]	-[9]	E
AID-A2 chimeras	#1 (19-57)	C	C	ND	ND	I
	#2 (59-84)	C	C+N	-	ND	I
	#3 (88-116)	C	N/C+N[3]	-	ND	I (?)
	#4 (118-150)	C	N/C+N[3]	-	ND	I (?)
	#5 (154-198)	C+N	C+N	2.7	-	I, R, E
	19-22	C	C+N	0.6	-	I
	25-28	C	N	ND	ND	-
	34-36	C	C+N	16	-	I
	39-42	C	N	2.3[11]	-[11]	-
	43-46	C	N	ND	ND	-
	50-54	C	C+N	-	-	I
	55-57	C	N	ND	ND	-
	#1 R178A	C	C	ND	ND	I
	#1 P182A	C	C	ND	ND	I
	#1 Y184A	C	C	ND	ND	I
	#1 Y184D	C	C	ND	ND	I
	#1 E185A	C	C	ND	ND	I
	#1 D187A	C	C	ND	ND	I
	#1 D188A	C	C+N	ND	ND	I, R
	#1 D187A/D188A	C	C+N	ND	ND	I,R
	#1 R190A	C	C	ND	ND	I
	#1 D191A	C	C	ND	ND	I
	#1 L198S	C	C>N/C	ND	ND	I, E
	#1 L196S/L198S	C+N	C+N	ND	ND	I, E, R

[1]The predominant phenotype (>80% of the cells) is indicated as C, mainly cytoplasmic; N, nuclear and C+N (when homogeneously distributed) or C>N (when still predominantly cytoplasmic but nuclear signal was clear).

[2] Determined by *E coli* assays except where specified. Normalized to wt AID = 1 in the same assay. ND, not determined.

[3] Phenotype in HeLa/293T cells for those constructs for which it was different.

[4] The activity determined by oligonucleotide cleavage assay of AID mutated at these positions but to different amino acids in ref [1] is shown for comparison.

[5] Hyper IgM patient mutation[2].

[6] Ref [3].

[7] Ref [4]

[8] Ref [5]

[9] Ref [6]

[10] The corresponding mutation in mouse AID was tested[7]

[11] Ref [8]

[12] Proposed subcellular localization mechanism affected in each construct, nuclear import (I), nuclear export (E) or cytoplasmic retention (R).

Supplementary Methods

AID modeling. To generate three-dimensional models of AID we used a homology modeling approach as implemented in the program MODELLER version 9v3 (ref [9]). We performed a structural alignment, using the models of APOBEC-2 (2NYT chains A and B, displaying alternative conformations in the α1/β1 turn; AID Arg19, structurally equivalent to A2 Glu60, might be critical in mediating a similar switch, but lacking experimental structural evidence we did not include any restraint with the predicted position of Zn^{2+} in the reaction center) and APOBEC3G (determined by X ray diffraction 3E1U, and by NMR 2JYW). We then generated a multiple sequence alignment of these three sequences with CLUSTAL W 2.0 (ref [10]) and manually corrected it according to the structural superposition. We then added the AID sequence to perform a final profile alignment on top of the first consensus, using structure-based penalties. We used this alignment in MODELLER 9v3 to build 20 AID models, from which the best scoring were selected (lowest final minimization energies and best fitting in terms of stereochemical quality criteria). JPRED prediction of secondary structure[11], results in good match of known A2 and APOBEC3G models; for AID, this prediction suggests the presence of alpha helices at the N- and C-termini (α1 residues 10-14 and α7 187-193, respectively). We added corresponding parameters in MODELLER to restrain these two alpha helical structures. α7 adopts a range of alternative positions relative to the globular core, since no homologous structure can be used as template; as spatial reference, one of these positions is shown in Figure 4 and Supplementary Figure 1 only with illustrative purposes. The dimer was generated by performing a structural superposition of the chosen monomeric model of AID, onto the dimer portion of A2 (2NYT). Including explicit hydrogen atoms in the riding positions, this initial dimer of AID was subjected to energy minimization protocols as implemented in the program CNS v1.2 (ref [12]) until convergence of energy values. The final model displays no clashes and good stereochemistry. Although the dimerization architecture needs definitive experimental support, it is used to spatially locate the areas corresponding to relevant residues in nuclear import, highlighting that their accessible surfaces join in a single continuous patch, juxtaposed in the dimer. Figures were prepared with PyMol v0.99 (http://www.pymol.org).

Cell transfections. We transiently transfected HeLa and 293T cells by using either the calcium phosphate precipitation or Lipofectamine 2000 (Invitrogen) according to the manufacturer instructions. Ramos cells were transiently transfected using Cell line nucleofector Kit V (Amaxa

Inc) and Amaxa electroporator as indicated by the manufacturer. Cells were used for assays and/or processed for imaging 24-36 h post transfection. We obtained stable transfectants of the Ramos B cell line by electroporation with pEGFP-N3 AID (250 V, 950 μF in 0.4 cm cuvettes) and selection in 2.5 mg ml^{-1} G418 (Wisent Inc, St-Bruno, Quebec).

Confocal microscopy and cell counting. Images were acquired using a Zeiss LSM 510 confocal microscope with excitation lasers Argon 488 nm (for EGFP and Alexa488) and HeNe 543 nm (for propidium iodide Alexa546) equipped with either 40X or 63X/1.4 oil immersion objectives. Saturation and background settings were adjusted before each session in the acquisition software provided by the manufacturer and all images acquired with the same settings. All experiments were repeated at least 2 times. Images were analyzed in ImageJ (Rasband, W.S., ImageJ, U. S. National Institutes of Health, Bethesda, Maryland, USA, http://rsb.info.nih.gov/ij/) and then transferred to Photoshop CS2 (Adobe Systems Inc) for cropping. Contrast was adjusted for the whole image in Photoshop when required to enhance visibility in the final figure without affecting the information registered in the original picture. Final figures were assembled in Illustrator CS2 (Adobe Systems Inc). To score subcellular localization we counted all cells, except those having mitotic figures or with saturated signal, in each of several randomly acquired fields from at least 2 independent experiments. Panels for which no quantitation is shown are representative of at least 85% of the transfected cells.

GST pull downs. GST fusion proteins were induced in *E coli* BL21 DE3 for 3 h at 37˚C with 0.5 mM IPTG. Cells were lyzed in PBS-KM (PBS 1mM $MgCl_2$ 3 mM KCl) 0.1% (v/v) Tween 20 by sonication. Lysates were clarified by centrifuging at 16,100 x *g* for 45 min at 4˚C and incubated for 2 h at 4˚C with 40 μl Glutathione-agarose resin (Sigma-Aldrich) pre-washed in PBS-KM 0.5% (w/v) BSA. Ramos B cells expressing AID-Flag or transiently transfected 293T cells were washed in PBS and extracted in Lysis Buffer for 30 min on ice. Cell extracts were clarified by centrifugation for 20 min at 15,000 x *g* at 4˚C and 3 x 10^6 293T or 2 x 10^7 Ramos cell equivalents mixed with 40 μl of GSH-sepharose beads loaded with ~5 μg of recombinant GST-fusion protein. Beads and extracts were incubated for 3 h at 4˚C with agitation, washed three times in PBS-KM and eluted for 20 min on ice in 50 μl of 20 mM reduced GSH 50 mM TrisHCl pH 8.0. The eluates and post-clearing lysates were separated in 10% SDS-PAGE, transferred to nitrocellulose, stained with Ponceau-S and probed with 1:3000 anti-EGFP-HRP (Miltenyi Biotec) or 1:1000 anti-AID followed by 1:5000 goat anti-Rat-HRP (Chemicon International).

Protein stability measurement. Transiently transfected 293T cells growing in 10 cm plates were harvested 36-48 h after transfection, resuspended in complete DMEM medium containing 100 μg ml^{-1} cycloheximide (Sigma-Aldrich) and replated in 6-well plates. One well was collected at 0, 1, 2, 4, 6 and 8 h after cycloheximide addition, washed with PBS and resuspended in Lysis Buffer for 30 min on ice. Cell extracts were clarified by centrifugation for 10 min at 4˚C, and the supernatants collected. Protein concentration of each sample was measured using the BCA Protein Assay Kit (Thermo Scientific). Volumes of lysate corresponding to 10 μg of protein for each time point were separated by SDS-PAGE and analyzed by western blot using anti-eGFP-HRP. Loading controls were probed by using anti-PCNA (1:2000 Abcam) or anti-Actin (1:5000 Sigma-Aldrich) followed by anti-mouse-HRP (Dako cytomation) or anti-rabbit-HRP (Dako cytomation), respectively.

AID decay in DT40 B cells was monitored by preincubating populations transduced with pMXs retroviral vectors encoding AID-GFP or AID D187A/D188A-GFP with cycloheximide for 1 h and then monitoring GFP signal by flow cytometry over time in the presence or absence of 10 ng ml^{-1} leptomycin B. Mean fluorescent intensity (MFI) of GFP was recorded and normalized to t = 0 to construct the decay curves.

Oligonucleotides. OJ 60, AAGGATCCCAAATGGACAGCCTCTTGATGAA, 5' AID, chimeras #1-5, BamHI; OJ 166, CGAATTCCCAAGTCCCAAAGTACGAAATGC, 3' AID, chimeras #1-4 EcoRI; OJ 196, NNGGATCCCAAATGGCCCAGAAGGAAGAGGCT, 5' APOBEC2 BamHI; OJ 197, NGAATTCCCCTTCAGGATGTCTGCCAACTTCT, 3’ AID-A2 #5 EcoRI; OJ 213, NNGAATTCTATGATGAGCACTTTTAAAGTTCT, 5' β-lactamase pUC18, EcoRI; OJ 214, NNGGATCCCCAATGCTTAATCAGTGAGG, 3' β-lactamase pUC18, BamHI; OJ 172, NNGAATTCTATGGGGGGTTCTCATCATCA, 5' lacZ pIND/lac, EcoRI; OJ 174, NNGGATCCTGATTTTTGACACCAGACCAACTG, 3' lacZ pIND/lac, BamHI. For C-terminal Flag tagging OJ 215, AATTCTGGAGACTACAAAGACGATGACGACAAGTCGGCCG-CTGGAGGATACCCCTACGACGTGCCCGACTACGCCTAGGC was annealed to OJ 216, GGCCGCCTAGGCGTAGTCGGGCACGTCGTAGGGGTATCCTCCAGCGGCCGACTTGTC GTCATCGTCTTTGTAGTCTCCAG; OJ 61, AAAAGCTTATCAAAGTCCCAAAGTA-CGAAA, 3’ AID for pTrc99a. To construct the Met-SV40 NLS OJ 190, CTAGCATGGGGG-CCCCCAAGAAGAAACGTAAAGTCA was annealed to OJ 191, GATCTGACTTTAC-GTTTCTTCTTGGGGGCCCCCATG. For Met-nucleoplasmin NLS OJ 192, CTAGCATG-

GCCAAGCGCCCTGCCGCCACTAAGAAGGCCGGTCAGGCCAAGAAGAAGAAGA was annealed to OJ 193, GATCTCTTCTTCTTCTTGGCCTGACCGGCCTTCTTAGTGGCGG-CAGGGCGCTTGGCCATG.

AID antisense to produce C-terminal truncations or mutations used in combination with OJ60: OJ 180, NNGAATTCCCGCACAGGTAGGTCTCACGCCGA, AID30; OJ 182, NNGAATTCCCT-GTAGCACTGTCACGCCTCTT, AID40; OJ 177, NNGAATTCCCGTTCTTATTGCGA-AGATAA, AID54; OJ 233, NGAATTCCCGCTCCAGGAGGTGAACCAGGT, AID85; OJ 234, NGAATTCCCGTTGGGGTTCCCTCGCAGA, AID103; OJ 235, NGAATTCCCTTTGAAGG-TCATGATGGCTAT, AID142; OJ 236, NGAATTCCCTTTGAAAGTTCTTTCATGGTT, AID160; OJ 181, NNGAATTCCCCAAAAGGATGCGCCGAAGCT, AID181; OJ 211, NNCGAATTCCCATCAACCTCATACAGGGGCA, AID187; OJ 204, NNGAATTCCCAGA-TCCCGAAGTACGAAATGCGT, L196S + L198S. AID sense used to produce N-terminal truncations in combination with OJ166, OJ 250, AAGGATCCCAAATGACCTACCTGTGC-TACGTAGT, AID 27-198; OJ 208, NNGGATCCATGGGCTGCCACGTGGAATTGCTCT, AID 55-198; OJ 306, AAGGATCCCAAATGCCCTGCTACGACTGTGCCCGA, AID 8$\tilde{6}$-198; OJ 307, AAGGATCCCAAATGAAGGCTGAGCCCGAGGGGCT, AID 120-198; OJ 308, AAGGATCCCAAATGACCTTCAAAGATTATTTTTACT, AI AID 140-198; OJ 309, AAGG-ATCCCAAATGGGGCTGCATGAAAATTCAGT, AID 164-198.

Oligonucleotides used together with their complementary for quickchange mutagenesis. OJ 241, CTGGGCTAAGGGTTGGCGTGAGACCTAC, R24W; OJ 246, GGATCTTCACCGCGGAC-CTCTACTTCTGTGAG, R112D; OJ 255, CAATTCAAAAATGTCGCCTGGGCTAAG-GGTCGGCG, R19A; OJ 268, CACCGCGCGCCTCGCCGCCTGTGAGGACCGCAAGGCTG, Y114A + F115A; OJ 270, CGCCTCTACTTCTGTTCCTCCCGCAAGGCTGAGCCCGAG, E117S + D118S; OJ 266, CCTTTTCACTGGACGCTGGTTATCTTCGCAATAAG, F46A; OJ 264, CCTTTTCACTGGACGCTGGTGCTCTTCGCAATAAGAACG, F46A + Y48A; OJ 194, CCTTTTCACTGGACGCTGGTGCTCTTGGCGCTAAGAACGGCTGCC, F46A + Y48A + R50G + N51A; OJ 276, CCTGTATGAGGTTGCTGCCTTACGAGACGCATTTCG, D187A-D188A; OJ 296, CTGTGCTACGTAGTGGAGGCGCAAGACAGTGCTACATCC, K34E/R35A/R36Q; OJ 290, GTATGAGGTTGATGCCTTACGAGACGCATTTC, D188A; OJ 304, CCTGTATGAGGTTGCTGACTTACGAGACGC, D187A; OJ 286, GCCCCTGTAT-GCGGTTGATGACTTACGAG, E185A; OJ 288, GACAGCTTCGGGCCATCCTTTTG-CCCCTG, R178A; OJ 292, GAGGTTGATGACTTAGCAGACGCATTTCGTAC, R190A; OJ

294, GTTGATGACTTACGAGCCGCATTTCGTACTTTG, D191A; OJ 184, CCTTTTGCCCC-TGGATGAGGTTGATGACTTACG, Y184D; OJ 278, CCTTTTGCCCCTGGCTGAGGTTGA-TGACTTACG, Y184A.

Supplementary References

1. Prochnow, C., Bransteitter, R., Klein, M.G., Goodman, M.F. & Chen X.S. The APOBEC-2 crystal structure and functional implications for the deaminase AID. *Nature* **445**, 447-51 (2006).
2. Revy, P. et al. Activation-induced cytidine deaminase (AID) deficiency causes the autosomal recessive form of the Hyper-IgM syndrome (HIGM2). *Cell* **102**, 565-75 (2000).
3. Shivarov, V., Shinkura, R. & Honjo, T. Dissociation of in vitro DNA deamination activity and physiological functions of AID mutants. *Proc Natl Acad Sci USA* **105**, 15866-71 (2008).
4. Ta, V. et al. AID mutant analyses indicate requirement for class-switch-specific cofactors. *Nat Immunol* **4**, 843-8 (2003).
5. Basu, U. et al. The AID antibody diversification enzyme is regulated by protein kinase A phosphorylation. *Nature* **438**, 508-11 (2005).
6. Doi, T. et al. The C-terminal region of activation-induced cytidine deaminase is responsible for a recombination function other than DNA cleavage in class switch recombination. *Proc Natl Acad Sci USA* (2009).
7. McBride, K.M., Barreto, V.M., Ramiro, A.R., Stavropoulos, P. & Nussenzweig, M.C. Somatic hypermutation is limited by CRM1-dependent nuclear export of activation-induced deaminase. *J Exp Med* **199**, 1235-44 (2004).
8. Conticello, S.G. et al. Interaction between antibody-diversification enzyme AID and spliceosome-associated factor CTNNBL1. *Mol Cell* **31**, 474-84 (2008).
9. Fiser, A. & Sali, A. Modeller: generation and refinement of homology-based protein structure models. *Methods Enzymol* **374**, 461-91 (2003).
10. Larkin, M.A. et al. Clustal W and Clustal X version 2.0. *Bioinformatics* **23**, 2947-8 (2007).
11. Cole, C., Barber, J.D. & Barton, G.J. The Jpred 3 secondary structure prediction server. *Nucleic Acids Res* **36**, W197-201 (2008).
12. Brunger, A.T. Version 1.2 of the Crystallography and NMR system. *Nat Protoc* **2**, 2728-33 (2007).